

Guangzhi Han  
Kang Huang ✉  
Yangshou Xiong  
Guodong Zhu  
Jiyou Peng

<https://doi.org/10.21278/TOF.482055022>

ISSN 1333-1124

eISSN 1849-1391

## AN ANALYSIS OF TIME-VARYING MESHING STIFFNESS OF HIGH CONTACT RATIO GEARS CONSIDERING A HIGH-ORDER MODIFICATION CURVE

### Summary

In this investigation into the technology of tooth profile modification, we analysed the impact of meshing, meshing shocks, and load distribution of high contact ratio gears in detail and explained the necessity of tooth profile modification so that a reduction in vibration and noise of high contact ratio gears can be achieved. Firstly, a design of a conventional profile modification curve is introduced, secondly, a new profile modification curve is derived from the transmission error calculated by using the slicing method, and thirdly, the time-varying meshing stiffness of gears with conventional and new profiles is calculated based on the finite element method. Finally, a comparative analysis of the time-varying meshing stiffness of gears shows that there exist a general effect of profile modification curves on the time-varying meshing stiffness of high contact ratio gears and an outstanding effect of the new profile modification curves on vibration and noise reduction. The paper also presents a new method for designing high contact ratio profile modification based on transmission error.

*Key words:* high contact ratio gears; profile modification; transmission error; time-varying meshing stiffness

### 1. Introduction

Gear is one of the important components of machinery and equipment, whose design and manufacturing technology represent the manufacturing level of a country to a certain extent. With the development of industry, high contact ratio (HCR) gears are more widely used and have become an important direction of research in the area of gear transmission. HCR gears have the advantage of smooth operation (like helical gears but without axial force) which greatly improves the load-carrying capacity. But there are also the problems of high sliding speed and sensitivity of tooth profile deviation, which leads to large vibration [1]. Due to the large contact ratio, the number of teeth involved in the simultaneous engagement of HCR gears is high, so different engagement regions alternate frequently. With the development of high-speed and heavy-load gear transmission, the vibration and noise levels of HCR gears will be further increased, which has become the key problem to be addressed in HCR gear transmission.

A large number of studies have shown that the gear transmission error is the main excitation factor of the vibration and noise in gear transmission systems [2-6]. Gear modification is an effective means of reducing the gear transmission system vibration and noise; many researchers have performed studies in this area. Bruyère et al. [7] reduced the transmission error of spur gears by tooth profile modification and verified the modification effect by applying dynamic analysis. Kim S et al. [8] established a helical gear static transmission error model considering gear modification and took the peak value of static transmission error as the optimization objective to optimize gear modification parameters, and studied the influence of modification parameters on gear transmission errors. Pedrero J I et al. [9] proposed a simple and efficient analytical model to analyze the influence of gear modification on gear meshing stiffness, transmission error and load distribution. The research results show that gear modification can reduce the amplitude of transmission error. In order to improve gear fatigue life, Jin T T et al.[10] established a gear tooth surface equation considering logarithmic modification, then calculated the contact stress and stress field at any position of the gear, and compared the contact stress before and after the modification, it was found that the logarithmic modification greatly reduced the contact stress on the tooth surface and reduced the stress concentration, thus increasing the fatigue life of the gear. Liu et al. [11] analysed the effect of different modification parameters on gear vibration from the perspective of time-varying meshing stiffness curves. Litvin et al. [12-13] reduced the magnitude of transmission errors of involute helical gears by triple modification of tooth surfaces applying the tooth contact analysis (TCA) technology. Pleguezuelos et al. [14] obtained the minimum peak-to-peak amplitude of the quasi-static transmission error and the tip relief of the minimum dynamic load by studying the effect of symmetrical long modification of the high contact ratio gear on the quasi-static transmission error. Also, based on both cases, the optimal modification length can be expressed by the function. Based on the multi-degree-of-freedom gear model, Velex, P. et al. [15] established a transmission error calculation model considering tooth profile modification. Fourier series is used to analyse the effect of tooth profile modification, the influence of modification parameters on transmission error is studied, and the general law of transmission error fluctuation of spur gear and helical gear with tooth profile is obtained. Jiang et al. [16] designed a diagonally modified tooth surface of helical gears, and the optimal modified tooth surface was determined by using a genetic algorithm with the objective of minimizing the magnitude of the transmission error and the root mean square of acceleration in the meshing direction. Yuan et al. [17] studied the effect of diagonal modification on the load distribution, comprehensive meshing stiffness, and transmission error of the tooth surface. Lee et al. [18] designed a 4th-order transmission error of internal concave spur gears and studied the machining simulation of the modified tooth surface of spur gears with a 4th-order transmission error. In addition, Ma et al. [19] explored the relationship between cutter error and accurate tooth profile for the benefit of gear modification design and contact performance studies. In this study, the triple modification is mainly carried out in the root, top, and both sides of the tooth, and the diagonal modification is carried out only in the mesh and meshing areas, and neither of them takes the overlap of the gear pair into account, while the effect of vibration damping is general.

Some scholars have also studied high-order modified curves of gears, but most of them focus on the ordinary involute tooth profile. Therefore, it is necessary to carry out a study of high-order modified curves of HCR gears. In this paper, the causes and peculiarities of the high contact ratio gear modification are analysed; then, the gear tooth deformation is deduced backwards from the transmission error; next, the deformation is fitted to the HRC gear tooth profile to obtain a seventh-order asymmetric tooth profile modification curve; finally, the time-varying meshing stiffness of conventional modified gears is compared with that of the high-order curved modified gears, which has important engineering practical significance for the design of high contact ratio gear modification and vibration reduction.

## 2. Tooth profile modification

### 2.1 Explanation of tooth profile modification

The transmission ratio of a gear pair should be stable and the base pitch of the two gears should be equal, based on the principle of gear meshing. In the case of HCR gear transmission, the alternation of the double-tooth meshing area and the three-tooth meshing area is mainly carried out. When the gear is driven, due to the manufacturing and installation error, elastic deformation after loading, thermal deformation, and other factors, the pitch of the driving wheel base circle is not equal to that of the driven wheel base circle, which causes the meshing interference phenomenon in the process of alternating meshing, which is also one of the main reasons for the vibration and noise in the gear transmission.

As shown in Fig. 1(a), when a pair of gears enters (leaves) the meshing position, the actual base pitch of the driving wheel is smaller than the actual base pitch of the driven wheel due to elastic deformation and other factors. Then, the gear pair comes into contact outside the theoretical meshing position. At this time, the top edge of the driven wheel will impact the root of the active wheel, or the top of the active wheel will scrape the root of the driven wheel. This results in a sudden increase in the ratio and a sudden increase in the engagement force at the point of engagement, which is known as geometric interference.

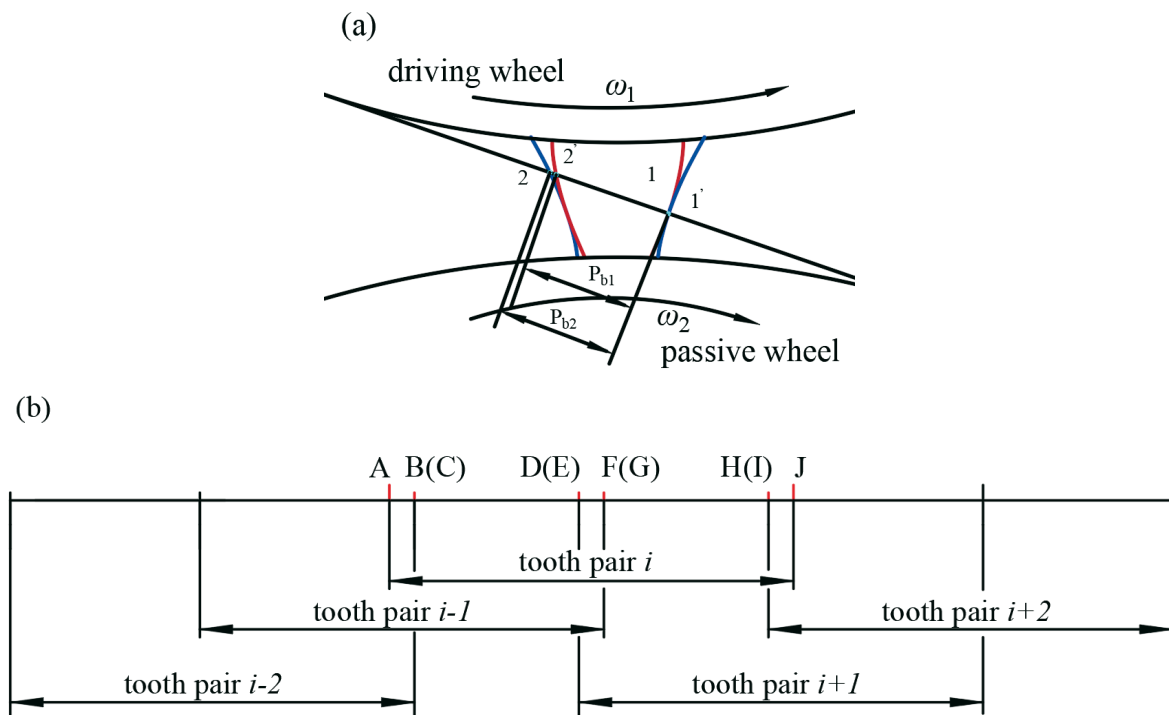


Fig. 1 Base circle pitch error and meshing state analysis

As Fig. 2 shows, since HCR gears alternate between double-tooth meshing area and three-tooth meshing area during the meshing process, there are load fluctuations. Points A, B, C, D, E, F, G, H, I, J) correspond to the points presented in Fig. 1(b). In this paper, the load distribution model proposed by Huang [20] based on the potential energy method was used to calculate the load distribution of high contact ratio gears. Fig. 2 shows the inter-tooth load distribution of a pair of HCR gears in one meshing cycle, which undergoes the alternating process of three teeth - double teeth - three teeth - double teeth - three teeth. The gear is meshing into the three-tooth area from point A. Points B and C, as well as points F and G, are the critical points between the three-tooth and double-tooth areas when the gear is about to mesh from the three-tooth area into the double-tooth area. Point D and point E, as well as

point H and point I are the critical points of the double-tooth area and the three-tooth area when the gear is about to mesh from the three-tooth area to the two-tooth area. When the gear enters the three-tooth meshing area from the two-tooth meshing area or enters the two-tooth meshing area from the three-tooth meshing area, it causes a sudden change in the meshing force of the gear at the meshing-in and meshing-out positions due to elastic deformation, which causes instantaneous shocks to the gear. The values of A and J in the first and third three-tooth meshing area of the meshing cycle are roughly 25% of the total load, and the values of B and I are roughly 28%; the values of C and H in the double-tooth meshing area are roughly 39% of the total load, whereas the values of D and G are roughly 62%; the values of E and F in the second three-tooth meshing area are 46%, the difference between E and D is 11%, and the difference between F and G is 16%, and there are large load fluctuations from D to E and from F to G.

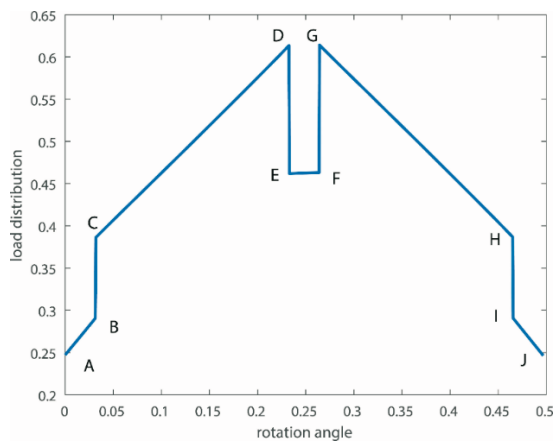


Fig. 2 Load distribution between teeth

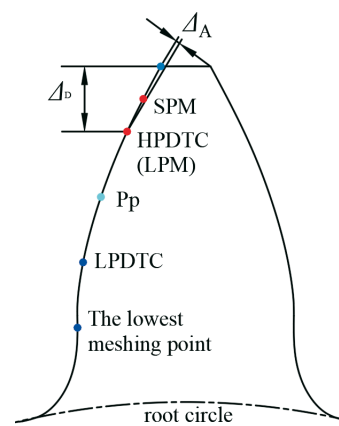


Fig. 3 Gear tooth model with tooth profile modification

Whether it is geometric interference or load fluctuation, these conditions are not conducive to gear transmission, especially for high-speed and heavy-load HCR gears. Nowadays, this kind of problem is solved by the tooth profile modification, i.e. by removing the geometric interference part of the material, so that the pitch of the driving gear and the base circle of the driven wheel are equal, and then the whole gear meshing process can be carried out smoothly.

## 2.2 Tooth profile modification

Tooth profile modification is a widely used method to reduce meshing shocks and load fluctuations by removing the material from the interfering part of the gear set so that the base circle pitch of the passive wheel and the base circle pitch of the driven wheel are equal. As a result, tooth profile modification can significantly improve the stability of mechanical transmission.

The gear model with tooth profile modification is shown in Fig. 3 [21]. HPDTC refers to the highest point of the double-tooth contact, LPDTC refers to the lowest point of the double-tooth contact, and Pp is the pitch point of the tooth. The tooth profile modification parameters mainly consist of three factors: the maximum profile modification amount  $\Delta_A$ , the length of profile modification  $\Delta_D$  and the modification curve form. As there is no unified formula for the calculation of the maximum modification amount, the following two methods are usually adopted to obtain the modification amount: (1) calculating the modification amount based on the deformation of the loaded teeth, and (2) gaining the modification amount according to the accuracy level of the pinion and gear. The position of the modification

starting point is determined by the length of the profile modification. In this study, two different tooth profile modification lengths are included, namely, the long profile modification (LPM) and the short profile modification (SPM). In the case of the long profile modification, the modification length corresponds to the highest point of the double-tooth contact (HPDTC); in the case of the short profile modification, the modification length corresponds to the midpoint of HPDTC and the highest point of the addendum. There are two positions of the tooth profile modification: tooth top modification and tooth root modification. There are also two ways of distributing the modification amount: concentrating on the main driving wheel or the driven wheel for modification and dividing the modification amount equally between the driving wheel and the driven wheel. In this paper, the tooth modification is carried out by modifying the tooth top and dividing the modification amount equally between the driving wheel and the driven wheel, which results in less weakening of the tooth root strength and tooth top strength.

The modification curve form is mainly determined by the following expression:

$$\Delta = \Delta_A \left( \frac{x}{\Delta_D} \right)^n \quad (1)$$

where  $x$  is the coordinate of the random contact point with the origin of the modification start point, and  $n$  is the index of the modification curve.  $n=1$  represents a straight-line modification, and  $n=2$  means a parabolic modification is used. In this paper, the kinetic response is analysed by using two kinds of modified curves (Fig. 4). In Fig. 4, S1 and S2 are straight-line long modified and straight-line segment modified curves, respectively, P1 and P2 refer to the parabolic long modified and parabolic short modified curves, respectively.

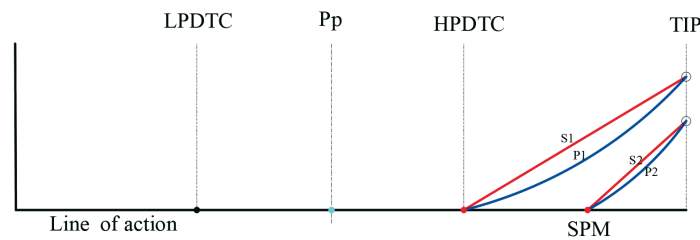


Fig. 4 Comparison of the tooth modification curves

The HCR gear parameters are shown in Table 1; the contact ratio  $\varepsilon$  of the gear is 2.132.

Table 1 High contact ratio gear parameters

Parameters	Values
Modulus $m$ (mm)	5
Pressure angle $\alpha$ ( $^\circ$ )	19
Number of teeth $z$	27/31
Tooth top height factor $h_a^*$	1.32
Top gap coefficient $c^*$	0.25
Tooth root fillet radius $r_0$ (mm)	0.25
Tooth width $B$ (mm)	20

### 3. Transmission error and new tooth profile modification curve

#### 3.1 Transmission error calculation

The transmission error is defined as the difference between an actual position of the driven gear and an ideal position. The ideal position refers to the position of the driven wheel when the driving and driven gears are both of ideal involute tooth shape and exhibit no elastic deformation (Fig. 5).

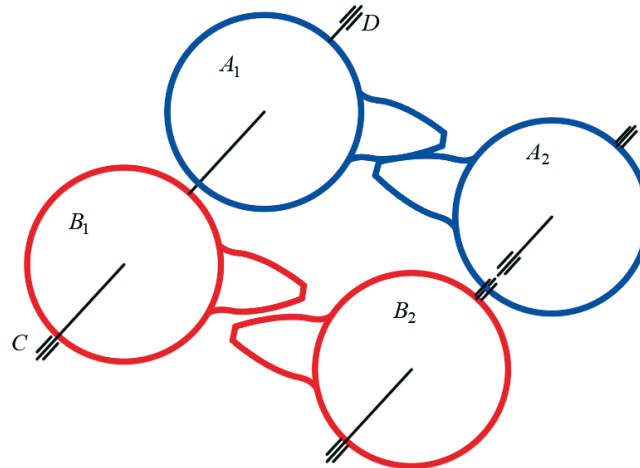


**Fig. 5** Transmission error concept diagram

A<sub>1</sub> and A<sub>2</sub> are ideal gears, B<sub>1</sub> and B<sub>2</sub> are actual gears, the ratios of both pairs of gear are 1, the two pairs of gear parameters are identical, A<sub>1</sub> and B<sub>1</sub> are fixed to the same rotating shaft, A<sub>2</sub> and B<sub>2</sub> are on different shafts, and the above-mentioned A<sub>1</sub> and B<sub>1</sub> gears, and A<sub>2</sub> and B<sub>2</sub> gears have the same parameters. When the shaft CD is rotated by a certain angle  $\theta_1$ , the difference between the rotation angle  $\theta_2$  of A<sub>2</sub> and the rotation angle  $\theta_2'$  of B<sub>2</sub> is the transmission error of the tooth pair ( $r_{b2}$  is the radius of B<sub>2</sub> gear base circle). The ideal involute gear transmission has no transmission error, in practice, due to load deformation, processing errors, assembly errors, and other factors, transmission error is inevitable. Therefore, the transmission error is calculated by the following expression:

$$TE = (\theta_2' - \theta_2) \times r_{b2} = (\theta_2' - \theta_1) \times r_{b2} \quad (2)$$

The aim of this paper is to propose a gear profile modification method for HCR spur gears and helical gears, so the transmission error of HCR gears is calculated by applying the slicing method [22], which is a numerical calculation method with short calculation time and high accuracy. The model of the transmission error calculation by the slicing method is shown in Fig. 6. It is assumed that the gear is decomposed into a number of mutually independent lamellae along the direction of the tooth width, with the same stiffness and thickness of each lamellae, and without considering the shear stress between each lamella.



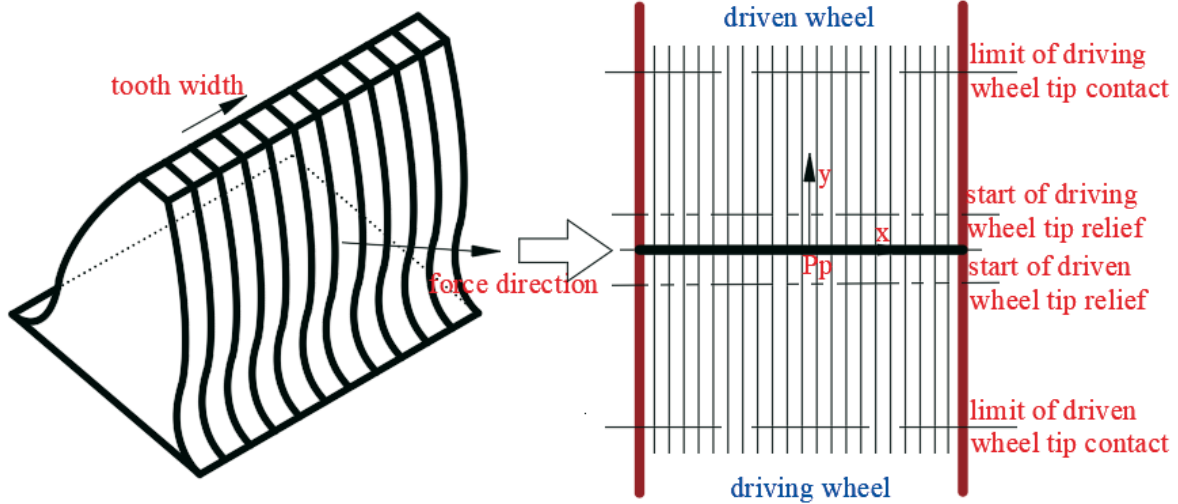


Fig. 6 Slicing method applied to the model of transmission error calculation

For an HCR gear pair, an  $xyPp$  coordinate system with the midpoint  $Pp$  of the tooth width as the coordinate origin is established in the meshing plane (Fig. 6), and the gear is divided equally into  $n$  lamellae along the tooth width direction, with each lamella having the same thickness, the same stiffness and the same design load ( $n$  is set to 1 because this is a study of a high contact ratio spur gear system). First, an initial deformation  $\delta_c$  is given in advance at the origin of the coordinates according to the design load, an initial interference amount  $\delta_0$  is provided, and then the coordinates of the engagement point of each piece are calculated as follows:

$$y = \frac{iP_t}{s} \quad (3)$$

where  $P_t$  is the pitch of the base circle,  $s$  is the number of steps in the meshing process divided by the engagement of one tooth in and out of the process, and  $i$  is one of the steps.

Then, the contact line interference is calculated for each slice as follows:

$$\delta(t) = \delta_c + \frac{\delta_0 |x|}{B} \quad (4)$$

where  $|x|$  is the distance of each slice along the  $x$ -axis direction to the coordinate origin and  $B$  is the tooth width.

Subsequently, the contact judgment is made for the position of each slice meshing point. There is the lowest point of meshing  $y_{\min}$  and the highest point of meshing  $y_{\max}$  in the gear meshing process. If the  $y$ -coordinate of the engagement point calculated above is not in this range  $[y_{\min}, y_{\max}]$ , it is judged that the slice is not engaged at this time. So, the calculated interference amount is set to 0 and the new amount of interference is  $\delta(t)'$ . After the contact judgment, all the interference amounts are summed up as follows:

$$\epsilon = \sum \delta(t)' \quad (5)$$

Next, the calculation of the average load for each slice is performed:

$$N = \frac{\epsilon k_0 B}{n} \quad (6)$$

where  $k_0$  is the pre-calculated gear stiffness.

Finally, the initial deformation is iterated. The iterative calculation is judged according to the design load, the calculated actual load, and the preset simulation accuracy, then, the final transmission error is obtained. The calculation process is shown in Fig. 7. Fig. 8 shows the final results of the calculated transmission errors:

$$\delta_c' = \delta_c - \frac{N - N_0}{N_0} \quad (7)$$

$$Q = \frac{N - N_0}{N_0} \quad (8)$$

where  $N_0$  is the design load and  $Q$  is the iterative judgment amount that ends the loop outputting the transmission error only when it is less than the preset iteration accuracy  $Q_0$ .

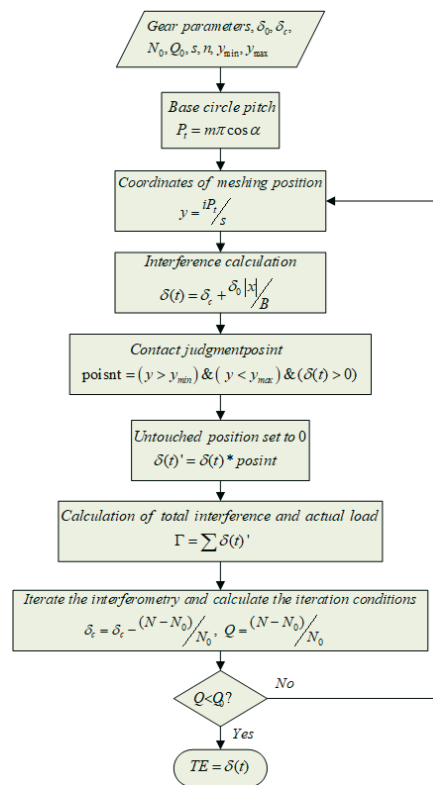


Fig. 7 Iterative calculation flow chart

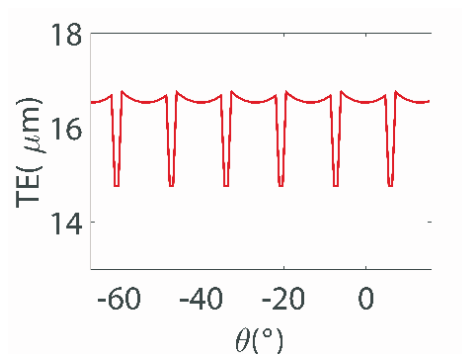


Fig. 8 HCR gearing errors



### 3.2 HCR gear deformation under load

Transmission error is the sum of the tooth profile error and the deformation under load. This paper intends to propose a tooth profile modification curve for high contact ratio gears based on the compensation of load deformation. Therefore, we need to calculate the margin of the transmission error by subtracting the tooth profile error. For this purpose, we establish a mechanical model of the transmission error (Fig. 9), and then solve the load deformation of HCR gears based on the existing transmission error [23].

In Fig. 9, the gear can be simplified as rigid involute teeth connected to the contact block and gear base through two springs; 1 and 2 are involute rigid teeth;  $B_1$  and  $B_2$  represent springs related to bending deformation, with stiffness coefficients  $K_{B1}$  and  $K_{B2}$ , and flexibility coefficients  $C_{B1}$  and  $C_{B2}$ , respectively;  $C_1$  and  $C_2$  represent springs related to contact deformation, with stiffness coefficients  $K_{C1}$  and  $K_{C2}$ , respectively, and flexibility coefficients  $C_{C1}$  and  $C_{C2}$ , respectively;  $A$  consists of two part groups representing the massless rigid body with two teeth in contact;  $P$  and  $G$  are gear base; the red line represents the ideal tooth shape, the blue line represents the actual tooth shape, and  $NM$  is the theoretical meshing line.

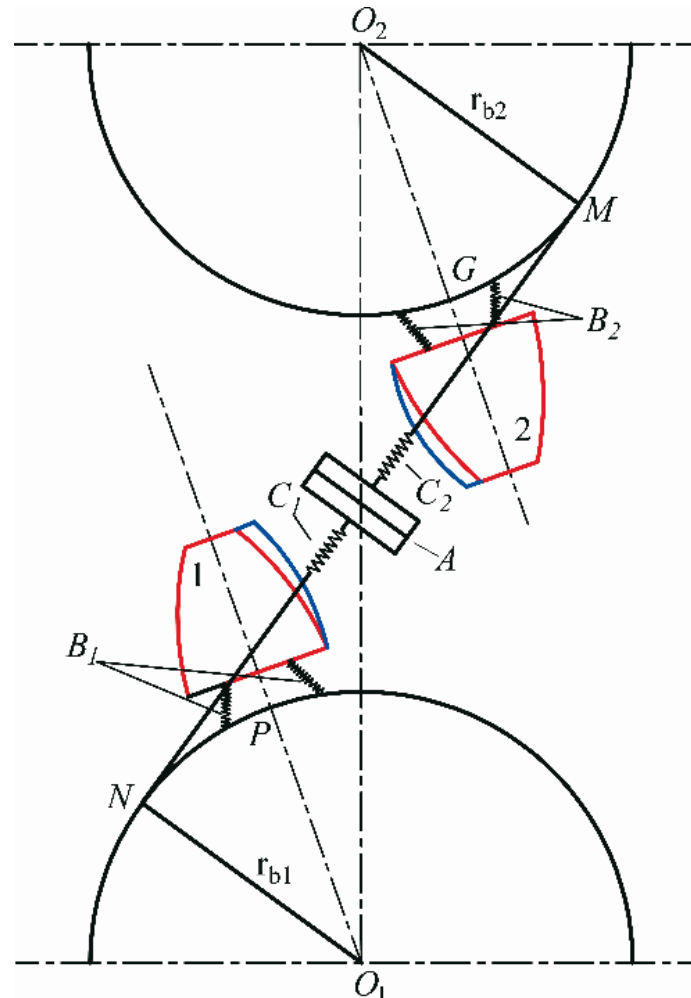


Fig. 9 Transmission error mechanics model

During gear transmission gears transmit motion and force through contact between gears. The elastic deformation at the point of contact in the direction of the force is the elastic bending deformation (EBD) of gear teeth and gear tooth contact deformation (GCD). In addition, it is also necessary to consider the tooth profile deviation  $E_f$  and tooth pitch deviation  $E_s$ .

The process of transferring force and motion from the driving wheel to the driven wheel is shown in Fig. 9 as follows: the force and motion have the driving wheel base P, passing through B<sub>1</sub>, rigid body involute teeth 1, C<sub>1</sub>, massless rigid block A, C<sub>2</sub>, rigid body involute teeth 2, B<sub>2</sub>, and driven wheel base G, and finally transferring the force and motion.

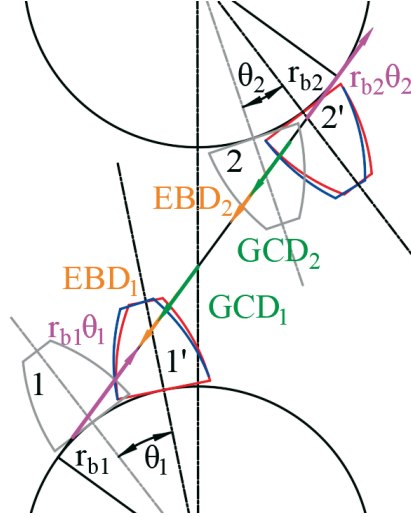


Fig. 10 Displacement calculation schematic

As shown in Fig. 10, if the driving wheel rotates at  $\theta_1$  for a certain period of time (from 1 position to 1' position), the displacement at the line of meshing is  $r_{b1}\theta_1$ . The driven wheel is rotated at an angle  $\theta_2$  (from 2 position to 2' position) and displaced along the line of meshing by  $r_{b2}\theta_2$ .  $EBD_1$  and  $GCD_1$  are the bending deformation displacement and contact deformation displacement along the meshing line at the engagement point of the driving wheel, respectively, and  $EBD_2$  and  $GCD_2$  are the bending deformation displacement and contact deformation displacement along the mesh line at the meshing point of the driven wheel, respectively. In addition, tooth pitch deviation  $ES$  and tooth profile deviations  $Ef_1$  and  $Ef_2$  are gear processing errors not indicated in the figure. It is stipulated that when the actual tooth pitch is greater than the nominal tooth pitch,  $ES$  is positive and the opposite is negative; when the actual tooth profile deviates to the outside of the ideal tooth entity,  $Ef$  is positive and the opposite is negative. Then the displacement of the driven wheel on the line of engagement is

$$r_{b2}\theta_2 = r_{b1}\theta_1 - EBD_1 - GCD_1 + Ef_1 + Ef_2 + ES - EBD_2 - GCD_2 \quad (9)$$

Then, due to the defining equation of the transmission error (2), it is known that

$$TE = Ef_1 + Ef_2 + ES - (EBD_1 + EBD_2 + GCD_1 + GCD_2) \quad (10)$$

Assuming that the normal load at this point is  $F_A$  and combining the data from Fig. 10, we obtain

$$\begin{cases} EBD_1 = F_A C_{B1} \\ EBD_2 = F_A C_{B2} \\ GCD_1 = F_A C_{C1} \\ GCD_2 = F_A C_{C2} \end{cases} \quad (11)$$

So, the total deformation produced by  $F_A$  is

$$EBD_1 + EBD_2 + GCD_1 + GCD_2 = F_A (C_{B1} + C_{B2} + C_{C1} + C_{C2}) = F_A \delta_A \quad (12)$$

where  $\delta_A$  is the integrated deformation flexibility coefficient of the meshing tooth pair at the meshing point, i.e. the amount of deformation along the direction of the meshing line under the action of unit load. Finally, the relationship between the transmission error and the deformation under load is derived as follows:

$$TE = E_A + F_A \delta_A \quad (13)$$

where  $E_A$  is the combined deviation including the tooth profile and the tooth pitch deviation.

### 3.3 New tooth profile modification curve based on deformation amount

Based on the above calculated gear deformation under load, the profile of gear deformation is inferred. HCR gears need to go through the meshing process of "three teeth-two teeth" from the gear teeth entering to the gear teeth exiting. As can be seen from Fig. 2, in most cases, the interdental load in the three-tooth meshing area is smaller than the interdental load in the two-tooth meshing area, thus the load deformation in the three-tooth meshing area is smaller than the load deformation in the two-tooth meshing area. In order to reduce the load fluctuation and reduce the impact, a new tooth profile modification curve (Eq. 14) is proposed based on the research done by Mu Y and He X [24]. At the same time, this paper considers the fact that the root part of the tooth profile modification will lead to a reduction in the root strength. Thus, the new tooth profile modification curve is a seventh-order double concave asymmetric parabola (the amount of tooth root modification is slightly smaller than the conventional root modification amount):

$$f(x) = a_0 + a_1x + a_2x^2 + a_3x^3 + a_4x^4 + a_5x^5 + a_6x^6 - a_7x^7 \quad (14)$$

$$\begin{cases} x = g_1, f(x) = \delta_1 \\ x = g_2 = g_3 - \lambda_1 m, f(x) = \delta_2 \\ x = g_2 = g_3 - \lambda_1 m, \frac{df(x)}{dx} = 0 \\ x = g_3 = r_{b1}, f(x) = \delta_3 \\ x = g_4 = g_3 + \lambda_2 m, f(x) = \delta_4 \\ x = g_4 = g_3 + \lambda_2 m, \frac{df(x)}{dx} = 0 \\ x = g_5, f(x) = \delta_4 \end{cases} \quad (15)$$

The parameters  $a_i (i=1 \sim 6)$  can be obtained by substituting Eq. 15 into Eq. 14 and solving the equation separately.  $a_7$  is used to reduce the root modification correction parameters, taking 0.0175-0.018 as the root part of the average value of the transmission error. The new tooth profile modification curve is shown in Fig. 10. In Eq. 15,  $g_i (i=1 \sim 5)$  is the coordinate of the rotational projection plane of the tooth surface in the tooth profile direction for coordinate point  $G_i (i=1 \sim 5)$ ,  $\delta_i (i=1 \sim 5)$  is the amount of modification of coordinate

point  $G_i$  in the tooth profile direction, the value of which is the above calculated deformation, but the tooth root modification amount is slightly smaller than the calculated actual deformation;  $\lambda_i$  ( $i=1\sim 2$ ) is the distance between coordinate points  $G_2$  and  $G_4$  and coordinate point  $G_3$  (meshing node) is used to define them.

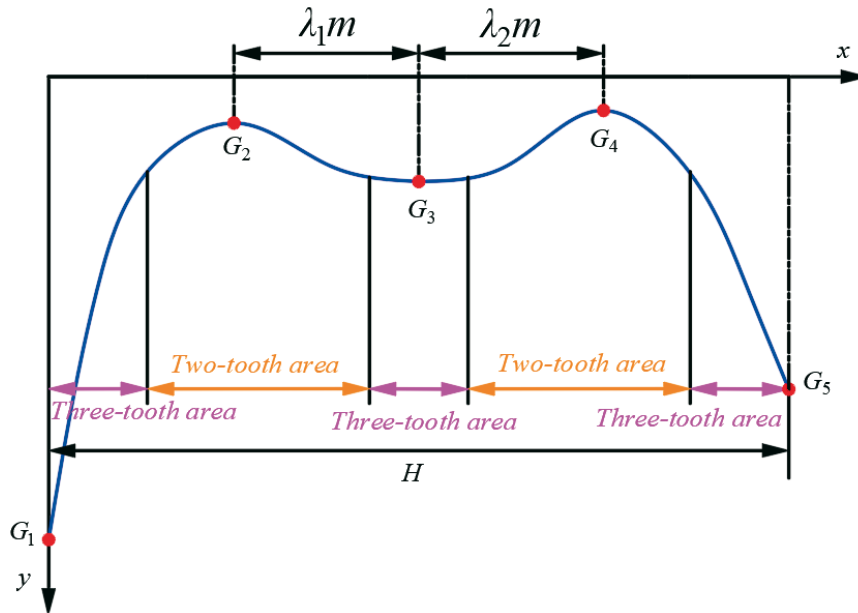


Fig. 11 Higher-order tooth profile modification curve

By comparing Fig. 4 and Fig. 11, it can be found that the main difference between the new profile modification method and the traditional modification method is the difference in the profile modification curve. In the new modification method, the tooth profile modification curve is a high-order modification curve, while in the traditional modification method, the tooth profile modification curve is mostly a straight line or a circular arc. Next, a comparative study of the new tooth profile trim curves and the conventional tooth profile trim curves will be conducted here.

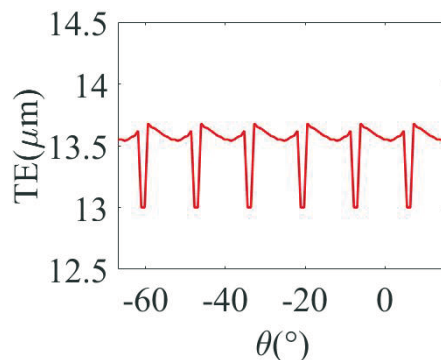


Fig. 12 Transmission error (high-order modification)

Applying the above high-order profile modification curve to the gears, the solved transmission error curve is shown in Fig. 12. Comparing Fig. 8 and Fig. 12, the magnitude and the average value of the gearing error with the high-order modification curve are smaller than that of the gearing error without the modification, so the high-order profile modification curve in this study can improve the gearing error.

#### 4. Time-varying meshing stiffness calculation and a comparative analysis

##### 4.1 Time-varying meshing stiffness

In this paper, the finite element analysis (FEA) method [25-26] is adopted to calculate the time-varying mesh stiffness of gears. First, the finite element contact model is established, and the finite element modelling process is as follows:

- 1) Build a finite element analysis mesh model [27] (Fig. 13);
- 2) Create a finite element analysis of the material properties: Young's modulus of steel  $E= 2.06\times 10^5$  MPa and Poisson's ratio  $\nu= 0.3$ ;
- 3) Create fixed constraints for the FEA models: All degrees of freedom of the inner hole points of the driven wheel are fixed. In addition, all degrees of freedom of the inner hole points of the driving wheel are also fixed except for the axial rotation;
- 4) Add load: Add design torque to the driving wheel;
- 5) Create tooth contact: The contact ratio of the high contact ratio gear is 2.132. To ensure that the finite element analysis can cover the whole meshing cycle, seven pairs of contacts are created to provide data for the later analysis.

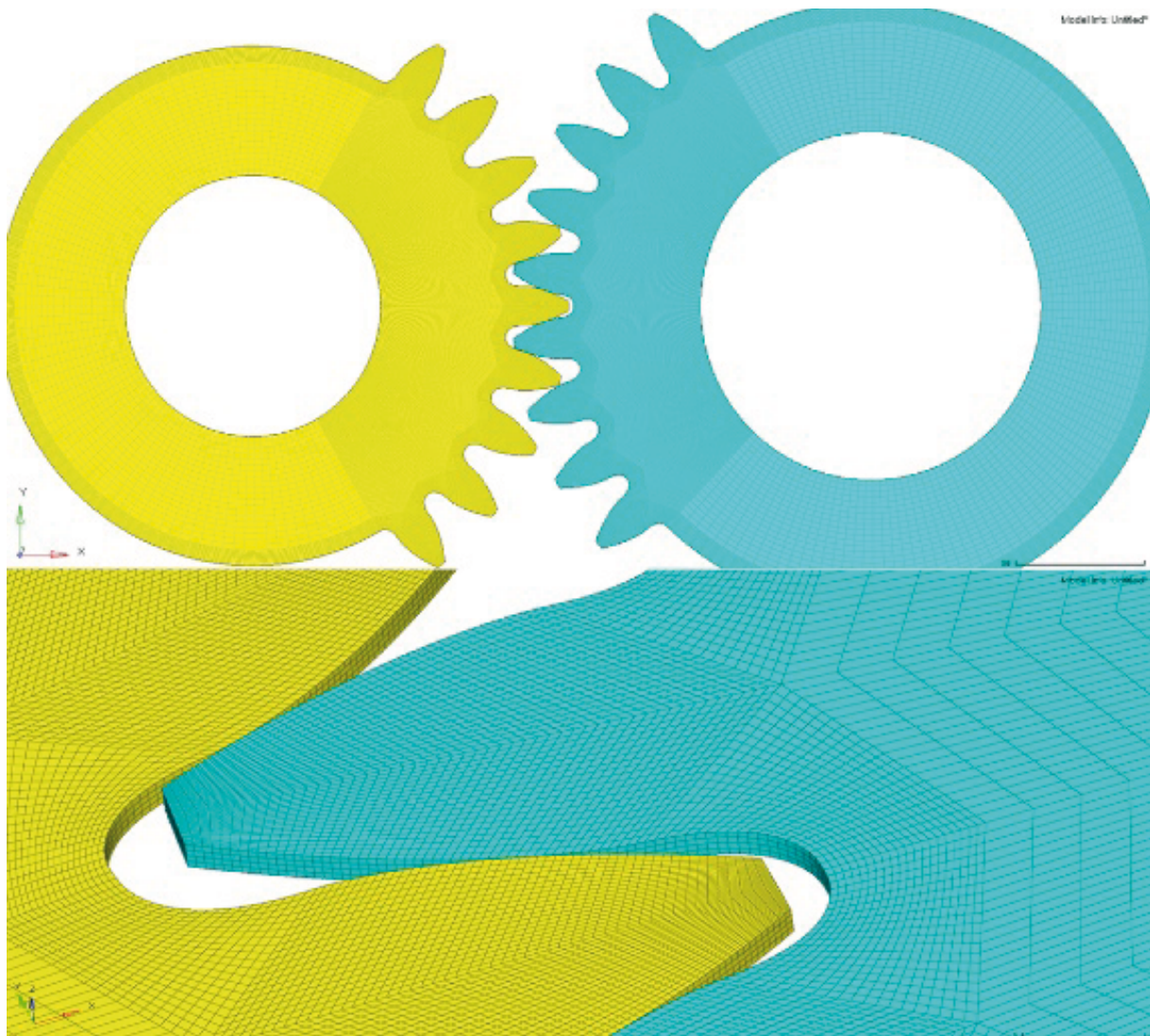


**Fig. 13** HCR gear mesh model



Subsequently, a finite element analysis is performed for the entire meshing cycle of the HCR gear, and the entire process of the gear from meshing to engagement is decomposed into a number of points covering the entire meshing cycle, and then the angular displacement  $\varphi$  at each contact position is obtained for the torsional stiffness  $\tau$  solution. Finally, the unit linear stiffness is obtained after equations (16), (17) and (18) are solved:

$$\tau = \frac{T}{\varphi} \quad (16)$$

$$k' = \frac{\tau}{r_{b1}} \quad (17)$$

$$k = \frac{k'}{B} \quad (18)$$

where  $T$  is the applied load and  $k'$  is the linear stiffness.

Due to the complexity of the HCR gear meshing process, the error of fitting the time-varying meshing stiffness by a Fourier series function is larger. Therefore, in this paper, the time-varying meshing stiffness is fitted in segments (two-tooth meshing area and three-tooth meshing area) as follows:

$$k(t) = \begin{cases} a_1(\text{mod}(t, T))^4 + a_2(\text{mod}(t, T))^3 + a_3(\text{mod}(t, T))^2 + a_4(\text{mod}(t, T)) + a_5, & 0 \leq \text{mod}(t, T) < T(\varepsilon - 2); \\ b_1(\text{mod}(t, T))^3 + b_2(\text{mod}(t, T))^2 + b_3(\text{mod}(t, T)) + b_4, & T(\varepsilon - 2) \leq \text{mod}(t, T) < T\varepsilon; \end{cases} \quad (19)$$

where  $T$  is the gear meshing period,  $t$  is the gear rotation time, and  $a_i$  and  $b_j$  are parameters, as shown in Table 2.

**Table 2** Eq. (19) fitting parameters

$a_i$	$b_j$
$a_1 = 4.788 \times 10^{-5}$	$b_1 = -1.823 \times 10^{-3}$
$a_2 = -7.191 \times 10^{-4}$	$b_2 = -1.3 \times 10^{-2}$
$a_3 = 1.8 \times 10^{-3}$	$b_3 = 5.683 \times 10^{-2}$
$a_4 = 6.854 \times 10^{-3}$	$b_4 = 20.5$
$a_5 = 16.65$	

The comparison of the meshing stiffness of each modification amount and the modification curve is shown in Fig. 14.



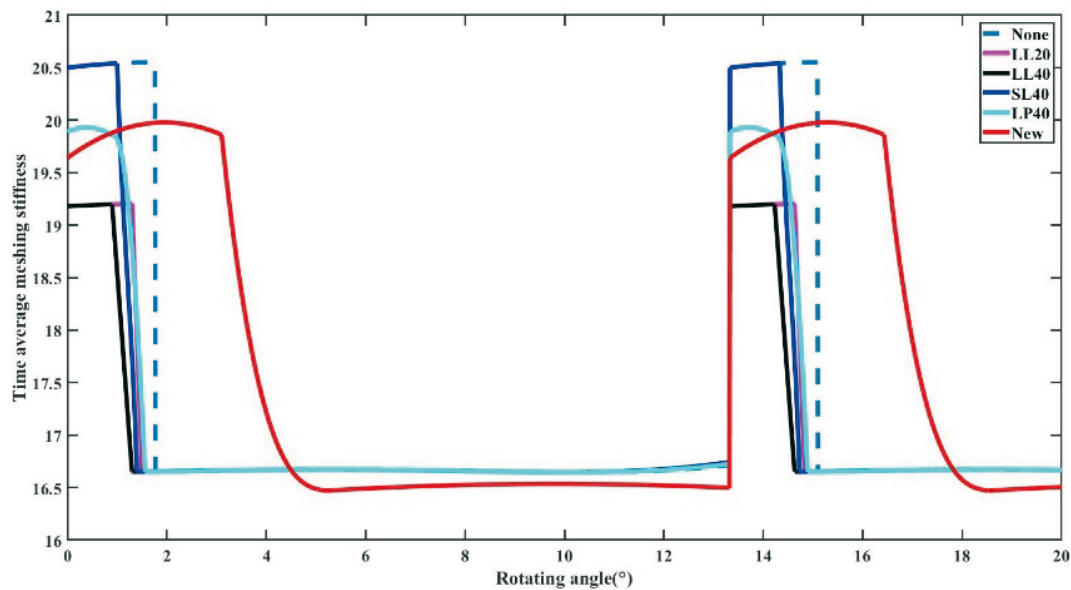


Fig. 14 Comparison of time-varying meshing stiffness

#### 4.2 Comparative analysis of time-varying meshing stiffness

In Fig. 14, None represents no tooth profile modification; LL20 represents a linear long modification with a modification of 20  $\mu\text{m}$ ; LL40 represents a linear long modification with a modification of 40  $\mu\text{m}$ ; SL40 refers to a linear short modification with a modification of 40  $\mu\text{m}$ ; LP40 refers to a parabolic long modification with a modification of 40  $\mu\text{m}$ ; and New uses a high-order modification curve modification.

The effect of the tooth profile modification on the stiffness is briefly analysed by comparing the stiffness curves. All the above time-varying meshing stiffness curves were obtained by applying the same load to the HCR gear pair. Comparing the curves of None, LL40 and SL40 (the same amount of trim and trim curves), when the HCR gear pair is not profile modified, the mesh stiffness changes steeply when the three-tooth meshing area alternates with the two-tooth meshing area. When the short modification is applied, the mesh stiffness of the three-tooth meshing area decreases, the gear teeth mesh smoothly and the stiffness changes more smoothly. When the long modification is applied, the three-tooth meshing area becomes significantly longer, the two-tooth meshing area is shortened, and the alternation between the two areas changes smoothly. The comparison of the two curves of LL20 and LL40 (the same trim curve) shows that the peak effect of different modifications on the stiffness is not significant, so the change in meshing stiffness is neglected. With an increase in the modification amount, the three-tooth meshing area becomes larger and the two-tooth area decreases. The comparison of the two curves of LL40 and LP40 shows that the three-tooth meshing area of the gear with the parabolic profile modification is slightly larger, but the stiffness is less reduced, so the alternation between the three-tooth meshing area and the two-tooth meshing area is smoother. In summary, the analysis of the New curve (high-order profile modification) shows that the modification curve makes the overall stiffness of the HCR gear slightly reduced, but greatly enlarges the three-tooth meshing area while the alternating stiffness of the two-tooth meshing area changes more smoothly, and then the transmission is smoother, which significantly reduces transmission noise and vibration.

## 5. Conclusion

The principle of gear profile modification is analysed and a new tooth profile modification curve is proposed by means of the calculation of the transmission error of HCR gears. In addition, the time-varying mesh stiffness of the gears with different modifications is solved by using the finite element method (FEM), and the following valid conclusions can be drawn:

- (1) The amount of modification will not change the peak of the time-varying meshing stiffness, but it will change the length of the three-tooth meshing area;
- (2) Compared to no modification and short modification, long modification will make the gear mesh out more smoothly, but it has less effect on the length of the tooth meshing area;
- (3) The comparison of the time-varying meshing stiffness of different modification curves shows that the parabolic modification is more flat than the linear modification in the three-tooth meshing area alternating with the two-tooth meshing area;
- (4) In the case of the new modification curve, the three-tooth meshing area becomes longer, that is, the contact ratio increases significantly. The alternation between the three-tooth meshing area and the two-tooth meshing area is smoother, thus greatly reducing vibration during operation;
- (5) The use of a high-order curve modification method based on the deformation of HCR gears under load can be proposed.

## Credit author statement

Kang Huang: Conceptualization, Project administration. Guangzhi Han: Writing - original draft, Writing - review & editing, Methodology. Yangshou Xiong: Software, Supervision. Guodong Zhu: Formal analysis. Jiyong Peng: Investigation.

## Acknowledgments

This study was supported by the National Natural Science Foundation of China (51775156), Natural Science Foundation of Anhui Province of China (1908085QE228), and Key Research and Development Project of Anhui Province (202004h07020013).

## REFERENCES

- [1] Anderson, N. E., and Loewenthal, S. H. Efficiency of Nonstandard and High Contact Ratio Involute Spur Gears, *ASME J.*, **1986**,108(1):113-126. <https://doi.org/10.1115/1.3260774>
- [2] Kang M R, Kahraman A. Measurement of vibratory motions of gears supported by compliant shafts, *Mechanical Systems and Signal Processing*, **2012**, 29: 391-403.<https://doi.org/10.1016/j.ymssp.2011.11.007>
- [3] Kang M R, Kahraman A. An experimental and theoretical study of the dynamic behavior of double-helical gear sets, *Journal of Sound & Vibration*, **2015**, 350:11-29. <https://doi.org/10.1016/j.jsv.2015.04.008>
- [4] Bozca M. Transmission error model-based optimisation of the geometric design parameters of an automotive transmission gearbox to reduce gear-rattle noise, *Applied Acoustics*, **2018**, 130: 247-259. <https://doi.org/10.1016/j.apacoust.2017.10.005>
- [5] Pedrero J I, Pleguezuelos M, Sánchez M B. Load sharing model for spur gears with tip relief, *Proceedings of the International Conference on Gears*, Munich, **2017**.
- [6] Pleguezuelos M, Sánchez M B, Pedrero J I. Control of transmission error of high contact ratio spur gears with symmetric profile modifications, *Mechanism and Machine Theory*, **2020**, 149: 103839. <https://doi.org/10.1016/j.mechmachtheory.2020.103839>

- [7] Bruyère J, Gu X, Velex P. On the analytical definition of profile modifications minimising transmission error variations in narrow-faced spur and helical gears, *Mechanism & Machine Theory*, **2015**, 92:257-272. <https://doi.org/10.1016/j.mechmachtheory.2015.06.001>
- [8] Kim S, Moon S, Sohn J, et al. Macro geometry optimization of a helical gear pair for mass, efficiency, and transmission error, *Mechanism and Machine Theory*, **2020**, 144: 103634. <https://doi.org/10.1016/j.mechmachtheory.2019.103634>
- [9] Pedrero J I, Pleguezuelos M, Sánchez M B. Analytical model for meshing stiffness, load sharing, and transmission error for helical gears with profile modification, *Mechanism and Machine Theory*, **2023**, 185: 105340. <https://doi.org/10.1016/j.mechmachtheory.2023.105340>
- [10] Jin T T, Wang J G, Jin S S, et al. Contact between Logarithmic Crowned Teeth of Spur Gear Transmission, *Applied Mechanics and Materials*, **2015**, 740: 69-78. <https://doi.org/10.4028/www.scientific.net/AMM.740.69>
- [11] Liu H, Zhang C, Xiang C L, et al. Tooth profile modification based on lateral-torsional-rocking coupled nonlinear dynamic model of gear system, *Mechanism and Machine Theory*, **2016**, 105:606-619. <https://doi.org/10.1016/j.mechmachtheory.2016.07.013>
- [12] Litvin F L, Gonzalez P I, Fuentes A, et al. Topology of modified surfaces of involute helical gears with line contact developed for improvement of bearing contact, reduction of transmission errors, and stress, *Mathematical and Computer Modelling*, **2005**, 42(9): 1063-1078. <https://doi.org/10.1016/j.mcm.2004.10.028>
- [13] Litvin F L, Fuentes A, Gonzalez-Perez I, et al. Modified involute helical gears: computerized design, simulation of meshing and stress analysis, *Computer methods in applied mechanics and engineering*, **2003**, 192(33-34): 3619-3655. [https://doi.org/10.1016/S0045-7825\(03\)00367-0](https://doi.org/10.1016/S0045-7825(03)00367-0)
- [14] Pleguezuelos M, MB Sánchez, Pedrero J I. Control of transmission error of high contact ratio spur gears with symmetric profile modifications, *Mechanism and Machine Theory*, **2020**, 149:103839. <https://doi.org/10.1016/j.mechmachtheory.2020.103839>
- [15] Velex, P., Bruyère, J., and Houser, D. R. Some Analytical Results on Transmission Errors in Narrow-Faced Spur and Helical Gears: Influence of Profile Modifications, *Journal of Mechanical Design*, **2011**, 133(3): 031010. <https://doi.org/10.1115/1.4003578>
- [16] Jiang J Fang Z, Wang F. Optimal design with diagonal modification for reducing design with diagonal modification for reducing helical gear noise, *Journal of Vibration and Shock*, **2014**, 33(7):63-67. <https://doi.org/10.13465/j.cnki.jvs.2014.07.011>
- [17] Yuan B, Chang S, Wu L, et al. Effect of cross modification on the quasi-static and dynamic characteristics of helical gear system, *Journal of Northwester Polytechnical University*, **2017**, 35(2). 232-239.
- [18] Lee C K. Manufacturing process for a cylindrical crown gear drive with a controllable fourth order polynomial function of transmission errors, *Journal of Mater Process Technology*, **2009**, 209(1): 3-13. <https://doi.org/10.1016/j.jmatprotec.2008.03.065>
- [19] Ma D, Liu Y, Ye Z, et al. Influence of Cutter Errors on Forming Accurate Variable Hyperbolic Circular Arc Tooth Trace Cylindrical Gears, *Transactions of FAMENA*, **2023**, 47(4): 13-31. <https://doi.org/10.21278/TOF.474044222>
- [20] Huang K, Sang M, Xiong Y, et al. Load Distribution in Meshing Process of Micro-segment Gears, *Forschung im Ingenieurwesen*, **2020**, 84:33-46. <https://doi.org/10.1007/s10010-019-00386-x>
- [21] Marković K, Vrcan Ž. Influence of tip relief profile modification on involute spur gear stress, *Transactions of FAMENA*, **2016**, 40(2): 59-70. <https://doi.org/10.1016/j.ymssp.2016.01.020>
- [22] He Z, Tang W, Sun S. A model for analysis of time-varying mesh stiffness of helical gears with misalignment errors, *Transactions of FAMENA*, **2021**, 45(2): 59-73. <https://doi.org/10.21278/TOF.452021720>
- [23] Tang J. A new model for gear transmission error calculation, *Mechanical Transmission*, **2008**,32(6):13-14. <https://doi.org/10.3969/j.issn.1004-2539.2008.06.004>
- [24] Mu Y, He X. Design and dynamic performance analysis of high-contact-ratio spiral bevel gear based on the higher-order tooth surface modification, *Mechanism and Machine Theory*, **2021**, 161: 104312. <https://doi.org/10.1016/j.mechmachtheory.2021.104312>

- [25] Vučković K, Čular I, Mašović R, et al. Numerical model for bending fatigue life estimation of carburized spur gears with consideration of the adjacent tooth effect, *International Journal of Fatigue*, **2021**, 153: 106515. <https://doi.org/10.1016/j.ijfatigue.2021.106515>
- [26] Kustura D, Vlak F, Matić T, et al. The Out-of-plane Static Analysis of Thin-walled Curved H-beams, *Transactions of FAMENA*, **2023**, 47(3): 61-78. <https://doi.org/10.21278/TOF.473053623>
- [27] Čular I, Vučković K, Galić I, et al. Computational model for bending fatigue life and failure location prediction of surface-hardened running gears, *International Journal of Fatigue*, **2023**, 166: 107300. <https://doi.org/10.1016/j.ijfatigue.2022.107300>

Submitted: 15.8.2022

Accepted: 05.12.2023

Guangzhi Han<sup>12</sup>

Kang Huang<sup>\*12</sup>

Yangshou Xiong<sup>13</sup>

Guodong Zhu<sup>12</sup>

Jiyou Peng<sup>12</sup>

<sup>1</sup> School of Mechanical Engineering, Hefei University of Technology, Hefei, China

<sup>2</sup> Anhui Province Key Laboratory of Digit Design and Manufacture, Hefei, China

<sup>3</sup> Anhui Province Key Lab of Aerospace Structural Parts Forming Technology and Equipment, Hefei, China

\*Corresponding author:

hfhuang98@163.com